A High-capacity MAC Protocol for UAV-enhanced RIS-assisted V2X Architecture in 3D IoT Traffic

Yaqi Mao, Xin Yang, Ling Wang, Dawei Wang, Osama Alfarraj, Keping Yu, *Senior Member, IEEE,* Shahid Mumtaz, *Senior Member, IEEE,* and F. Richard Yu, *Fellow, IEEE*

***Abstract*—With the development of internet of things (IoT) technology and its wide application in urban traffic, the next-generation vehicle-to-everything (V2X) communication network should support high-capacity, ultra-reliable, and low-latency massive information exchange to provide unprecedentedly diverse user experiences. The development of the sixth-generation (6G) mobile communication technology will pave the way for realizing this vision. Reconfigurable intelligent surfaces (RISs), a critical 6G technology, is expected to make a big difference in V2X communications when used in conjunction with unmanned aerial vehicles (UAVs), allowing for extremely increased communication capacity and reduced latency. We propose a UAV-enhanced RIS-assisted V2X communication architecture (UR-V2X) suitable for urban three-dimensional (3D) IoT traffic and design an adapted MAC protocol UR-V2X-MAC to accomplish communication resource allocation and scheduling. The UAVs are used as access points and resource allocation centers, while the RISs are used as passive relays to assist V2X communication in proposed architecture. To improve the performance of UR-V2X-MAC, we use a distributed optimization algorithm in the message report phase of the protocol to maximize the system capacity by allocating the transmit power and alternately optimizing the RIS phase shift matrix. We analyze the delay and system capacity characteristics under different parameter settings through theoretical derivation and protocol performance simulation. Analysis and simulation results are presented to demonstrate that UR-V2X-MAC achieves a reduction in communication delay and a significant increase in system capacity through detailed design and alternate optimization compared to the existing V2X MAC protocol and no-RIS case.**

This work was supported in part by the National Natural Science Foundation of China under Grant No. 62271412, 62271399, 62071250, partly supported by Natural Science Basic Research Plan in Shaanxi Province of China under grant No. 2022KJXX-39, in part by the 6G-SENSES project from the Smart Networks and Services Joint Undertaking (SNS JU) under the European Union's Horizon Europe research and innovation programme under Grant Agreement No 101139282, and supported by the Distinguished Scientist Fellowship Program (DSFP) at King Saud University, Riyadh, Saudi Arabia. *(Corresponding author: Xin Yang and Keping Yu).*

Yaqi Mao, Xin Yang, Ling Wang and Dawei Wang are with the School of Electronics and Information, Northwestern Polytechnical University, Xi'an 710072, China (e-mail: maoyq@mail.nwpu.edu.cn; xinyang@nwpu.edu.cn; lingwang@nwpu.edu.cn; wangdw@nwpu.edu.cn).

Osama Alfarraj is with the Computer Science Department, Community College, King Saud University, Riyadh 11437, Saudi Arabia (email:oalfarraj@ksu.edu.sa).

Keping Yu is with the Computer Science Department, Community College, King Saud University, Riyadh 11437, Saudi Arabia, and with the Graduate School of Science and Engineering, Hosei University, Tokyo 184-8584, Japan (email: KepingYu@ksu.edu.sa; keping.yu@ieee.org).

Shahid Mumtaz is with Department of Applied Informatics, Silesian University of Technology, Akademicka 16 44-100 Gliwice, Poland and Departement of Computer Sciences, Nottingham Trent University, UK. (email: Dr.shahid.mumtaz@ieee.org).

F. Richard Yu is with the Department of Systems and Computer Engineering, Carleton University, Ottawa, ON K1S 5B6, Canada (e-mail: richard.yu@carleton.ca).

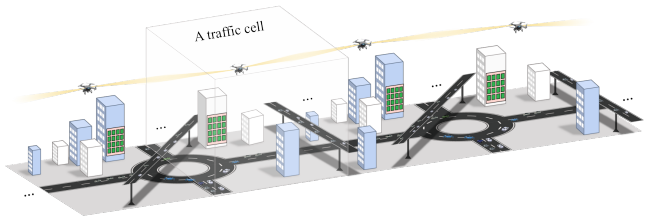

Fig. 1. An illustration of the UR-V2X application scenario.

***Index Terms*—Medium access control (MAC), vehicle-to-everything (V2X), UAV communications, reconfigurable intelligent surface (RIS).**

I. Introduction

With the development of the fifth-generation (5G) mobile communication, the Internet of things (IoT), big data, and other technologies, urban intelligent transportation has made great progress. Vehicle-to-everything (V2X) communication, as the backbone of the intelligent transportation system (ITS), has received extensive attention from researchers and is in the process of rapid advancement [1].

V2X is a generic term that covers multiple forms of internet of vehicles (IoV) communication such as vehicle-to-vehicle (V2V), vehicle-to-infrastructure (V2I), and vehicle-to-pedestrian (V2P) [2]. The challenges faced by V2X application scenarios are mainly in the following two aspects. On the one hand, there is a three-dimensional trend in urban transportation construction to cope with the increasing number of intelligent connected vehicles (ICVs). The increasing number of buildings and overpasses cause serious obstacles to communication, leading to a decrease in system capacity. On the other hand, the massive information interaction brought about by the development of Beyond 5G (B5G) and sixth-generation (6G) technology puts unprecedentedly high demands on communication delay.

Therefore, the intervention of emerging communication methods is imminent. Unmanned aerial vehicle (UAV) communication and reconfigurable intelligent surfaces (RISs) are critical technologies for 6G. In this paper, we propose a UAV-enhanced RIS-assisted V2X communication architecture (UR-V2X) and design a UR-V2X MAC protocol (UR-V2X-MAC) suitable for urban three-dimensional (3D) traffic, aiming to overcome the above challenges.

UAVs are highly flexible, low-cost, and easy to deploy. They can provide temporary coverage when the ground infrastructure is overloaded on congested roads or during rush

hours in V2X architecture. The UAVs used in UR-V2X we proposed can form line-of-sight (LoS) propagation paths with ground-based ICV terminals with a higher probability than roadside units (RSU) or base stations (BSs) in conventional V2X architectures. Meanwhile, to break through the limitation of the communication range of a single UAV, multiple UAVs can be used to collaborate and thus provide wider coverage of V2X services.

RIS has recently been recognized as a promising technology to effectively improve the propagation environment on demand. RIS is a meta-surface equipped with low-cost integrated electronic circuits that can be programmed to alter an incoming electromagnetic field in a customizable way [3]. A typical architecture of RIS consists of three layers and a controller. In the outer layer, a large number of metallic patches called elements are printed on a dielectric substrate to directly interact with incident signals. A PIN diode is embedded in each element, which can be switched between "On" and "Off" states to generate a phase-shift difference of π in rad by controlling its biasing voltage via a direct-current feeding line. In the middle layer, a copper plate is used to avoid the signal energy leakage. The inner layer is a control circuit board that is responsible for adjusting the reflection amplitude/phase shift of each element, triggered by a smart controller attached to the RIS. Different phase shifts of elements can be realized independently via setting the corresponding biasing voltages by the smart controller. In practice, field-programmable gate array (FPGA) can be implemented as the controller to communicate and coordinate with other network components (e.g., BSs and users) through separate wireless links for information exchange with them. Moreover, RIS can be easily integrated into urban communication environments as its hardware footprint is very small and can be easily deployed on building facades, rooms, factory ceilings, etc [4].

The simultaneous utilization of RIS and UAV in the proposed UR-V2X creates an innovative space for providing massive communication services to ICVs. The UAV acts as an access point (AP), providing core network access for ICVs, and the RIS facilitates information interaction between ICVs through passive beamforming. Furthermore, by integrating RIS into the communication process, problems such as obscured LoS paths and high energy consumption of UAVs can be mitigated, which improves the quality of the wireless channel. In addition, UAVs can extend the communication capabilities of RIS for ICVs through resource allocation and phase control.

As one of the cores of V2X communication, the medium access control (MAC) protocol determines the allocation, intervention, and scheduling of resources in the network. The design of MAC protocols is a major determinant of network performance. In practical scenarios, transmission conflicts and unfair allocation of channel resources often occur, which need to be coordinated by the MAC protocol. Moreover, the predictable mobility of ICVs, the coordinated working of UAVs and RISs, and the reservation and allocation of multidimensional resources should be taken into account when designing MAC protocols for UR-V2X to provide high-quality V2X communication services. With all these consideration factors, there is still a significant amount of work to be done to improve the design of MAC protocols for V2X communication systems.

The contributions made in this paper can be summarized as follows.

1) We propose a UAV-enhanced RIS-assisted V2X architecture, or UR-V2X for short, to cope with the challenges posed to communications by the increase in obstacles and the increase in communication services in 3D urban traffic.
2) Then, we design the UR-V2X-MAC protocol adapted to the UR-V2X architecture to accomplish communication resource allocation and scheduling. The UAVs are used as APs and resource allocation centers, and the RISs are used as passive relays to assist V2X communication. The allocation of time and channel resources and the formats for the different types of frames are described in the protocol. The algorithm flow of UR-V2X-MAC is given in the paper.
3) In order to enhance the performance of UR-V2X-MAC, we model the optimization problem to maximize the system capacity by distributing the alternating optimization of transmit power and RIS phase shift matrix.
4) Finally, we analyze the delay and system capacity characteristics under different parameter settings through theoretical derivation and protocol performance simulation. The simulation results are also compared with existing V2X MAC protocols and RIS-free solutions to verify the advancement of UR-V2X-MAC. Our results unveil that a) the time required to acquire a time slot using UR-V2X-MAC is shorter than using VeMAC [5] when the number of competing ICVs is the same; b) UR-V2X-MAC reduces the V2V packet delay and message delay compared to the scheme without RIS. Meanwhile, the reduction effect becomes significant with increasing the number of groups of RIS, especially in the case of large V2V distance; c) there is an increase in system capacity with the addition of reflecting elements compared to the access scheme without RIS.

The rest of the paper is organized as follows. Section II describes the related work on UAV and RIS-assisted communication and VANET-oriented MAC protocols. Section III builds a system model for UAV-enhanced RIS-assisted V2X architecture. Section IV describes the designed UR-V2X-MAC protocol in detail with protocol flow and optimization algorithm. Section V analyzes the delay and system capacity performance under UR-V2X-MAC. Section VI gives the simulation results of the above performance through several comparative experiments. Finally, we summarize this paper and look forward to future work.

II. Related Works

In this section, we introduce some recent research advances in UAV-assisted communication and RIS-assisted communication in VANET. In addition, the special requirements imposed by VANET on MAC protocols are analyzed and several typical MAC protocols for VANET are introduced.

A. UAV-assisted Communication

Over the past few years, there has been considerable focus on utilizing IoT devices to improve wireless network performance. One specific area of interest is the use of UAVs to enhance the connectivity of ITSs' core vehicular networking infrastructure. This aims to enhance the functionality and operability of various innovative in-transit digital services, as evidenced by numerous publications in the literature.

UAVs are highly flexible, low-cost, and easy to deploy. They can provide temporary coverage when the ground infrastructure is overloaded on congested roads or during rush hours in V2X architecture [3], [6]. Al-Hilo *et al.* [7] presented a UAV-assisted data dissemination model in VANETs with either overloaded or unavailable communication infrastructure and proposed a proximal policy optimization algorithm to solve the problem of UAV trajectory, radio resource, and caching replacement with the objective of maximizing the energy efficiency of the UAV. Su *et al.* [8] studied a content distribution mechanism between UAVs and vehicles and implemented a coalition game to solve an optimization problem of data distribution with the objective of minimizing the transmission delay. The UAVs used in UR-V2X we proposed can form LoS propagation paths with ground-based ICV terminals with a higher probability than roadside units (RSU) or base stations in conventional V2X architectures. Meanwhile, to break through the limitation of the communication range of a single UAV, multiple UAVs can be used to collaborate and thus provide wider coverage of V2X services. Considering anticollision and communication interference in the multi-UAV enabled VANETs, Liu *et al.* [9] investigated a problem of jointly optimizing vehicle communication scheduling, UAV power allocation, and UAV trajectory. Zhou *et al.* [10] proposed a cooperative vehicular networking framework that enables the formation of an airborne backbone network consisting of UAVs, which assists in ground-based vehicular communications. Oubbati *et al.* [11] examined the feasibility of using UAVs in ad hoc mode to improve data routing among ground vehicles, thereby enhancing the data delivery ratio. They also introduced a UAV-assisted routing protocol in [12], which incorporates a predictive routing path lifetime estimation technique. The reported results demonstrated a significant improvement in performance for the UAV-assisted vehicular ad hoc network (VANET), as evidenced by reduced end-to-end delay and improved data delivery ratio. Clustering has traditionally been employed to enhance connectivity in urban VANETs (e.g., [13]). In contrast, Abualola *et al.* [14] proposed a method to enhance the performance of urban IoV by selecting stable relays and opportunistically using UAVs. Ghazzai *et al.* [15] aimed to identify the optimal deployment locations for UAVs, considering constraints such as intervention time and UAV battery lifetime, in order to maximize network coverage. Samir *et al.* [16] investigated network performance in a vehicular network operating under severe conditions, with limited availability of RSUs due to destruction or overload. The authors presented an optimization framework for joint trajectory and radio resource allocation to maintain a certain service rate threshold for each vehicle. Additionally, Samir *et al.* [17] examined the total number of UAVs required to meet the navigation requirements of vehicles along a road, taking into account specific delay constraints.

B. RIS-assisted Communication

RIS has recently been recognized as a promising technology to effectively improve the propagation environment on demand. RIS is a device made of low-cost meta-surfaces that can reflect or refract incident signals, thereby manipulating the propagation of electromagnetic waves [18]. These meta-surfaces are thin transparent or translucent materials that can be easily deployed in any type of environment, whether indoors or outdoors [19], [20]. This helps the communication network to meet the LoS requirements between the sender and receiver. It also facilitates the transmission of signals with high quality, even in the presence of numerous obstacles. RIS is passive and performs only reflection functions, unlike the relays that can enhance the signals.

There is a growing interest in utilizing RISs to enhance wireless links and improve spectral and energy efficiency [21]. However, the exploration of RIS-assisted V2X is still in its early stages. Previous studies have acknowledged the crucial role of RISs in enhancing vehicular networking [22], [23]. Specifically, by appropriately allocating resources and adjusting RISs coefficients, significant capacity improvements can be achieved in V2I communication [22]. Moreover, the strategic placement of RISs can effectively address the challenges posed by high path loss in higher frequency bands, thereby enhancing V2X connectivity [23]. Furthermore, the deployment of RISs can extend the transmission range by facilitating communication even in non-line-of-sight (NLoS) scenarios [24]. These versatile benefits offered by RISs bring about tremendous potential and create new possibilities for advanced V2X applications outlined in Rel. 16 [25], such as autonomous driving, queue driving, and extended sensors with highly demanding Quality of Service (QoS) requirements, including high data rates, extensive coverage, ultra-low latency, and minimal outage probability. Pan *et al.* [26] proposed a communication system for VANETs that combines artificial intelligence (AI) and RIS technology. This system focuses on enhancing energy efficiency while ensuring low transmission latency in VANETs. To achieve this goal, the team developed a model that maximizes energy efficiency and simultaneously optimizes the settings of all participants, resulting in efficient and timely communication.

C. VANET MAC Protocol

VANET is currently being integrated with cellular networks. VANET schemes based on global unified regulations of architecture and communication protocols, and Long Term Evolve-vehicle (LTE-V) technology based on data interaction standards began to emerge. VANET is evolving in the direction of V2X.

The main research objective of the MAC protocol of VANET is to guarantee the timeliness and reliability of service transmission. If the timeliness is too low, it may cause the safety information not to be delivered in time which leads to

accidents, or the application information not to be delivered in time which leads to poor user experience. If the reliability is not strong, it will lead to inaccurate or undeliverable information, which will cause an unpredictable impact on a series of subsequent behaviors or judgments of vehicles.

Traditional contention-based MAC protocols are not well suited to meet the stringent QoS requirements of vehicular networking applications. Researchers have proposed several improved MAC protocols with the main idea of adaptive optimization of CW-based protocol parameters. Factors such as network congestion state or node density can be used to optimize the CW so that the nodes can access the wireless channel more reliably. Mao *et al.* [27] investigated the estimation of node density to aid in the optimization of CW. In addition to CW, other parameters such as transmit power can also be adaptively optimized to improve protocol performance.

In vehicular networks, reservation-based MAC protocols typically use time division multiple access (TDMA), space division multiple access (SDMA), or code division multiple access (CDMA) access channels. Most of the research has focused on TDMA-based protocols. VeMAC [5] is a typical TDMA-based distributed MAC protocol that divides all the time slots in a frame into three time slot subsets, and the left and right moving vehicles and roadside units (RSUs) select the time slots in the corresponding time slot subsets. PTMAC [28] allows the nodes to detect the potential time slot collisions so that the time slot substitution can be performed in advance. CTMAC [29] dynamically selects idle nodes to forward data. EVC-TDMA [30] allows nodes to dynamically select relay nodes based on relative speed and buffer length. Deng *et al.* [31] utilize relative distances between nodes to allocate time slots.

D. Joint use of UAV and RIS

The joint use of UAV and RIS can create favorable conditions for signal propagation and extend communication coverage. The combination of the two can provide high-capacity, high-reliability communications, which can help realize a series of 6G network use cases and applications represented by IoV. Existing work on the joint use of UAVs and RISs includes three main types in terms of application forms: 1) RISs are mounted on UAVs to assist in communications; 2) UAVs carry RISs to assist in communications while doing relaying; and 3) UAVs collaborate with RISs mounted on walls or other fixed surfaces. In almost all exiting paper on the joint use of UAV and RIS, the authors focus on finding a solution to a particular problem by optimizing various parameters such as UAV velocity, altitude, maneuverability, RIS phase shift, user assignment, beam formation, etc. and using the optimal technique to achieve the solution. For each of these three types of application forms, some representative UAV and RIS joint use efforts from recent years are described below.

In the first category of research, UAVs are solely considered as RIS carriers. This type of joint usage is mostly used in mobile edge computing (MEC) systems [32]–[34] or is used for throughput enhancement in communication networks [35]. In [33], the energy efficiency of the MEC system with the assist of UAV-mounted RIS is maximized by jointly optimizing user scheduling, input bits, CPU cycling frequency, and the trajectory and phase-shift design. Zhai *et al.* [34] proposed the use of the UAV, acting as both MEC server and relaying RIS for the ground MEC, to minimize the total energy consumption of the system. The performance of wireless communication systems based on airborne RIS was studied and analyzed in [35]. This work investigates for the first time the impact of different shadowing conditions in an airborne communication system also supported by a RIS and compares the performance of the considered system with that of decoding and forward relaying, thus highlighting the advantages of combining RIS with UAV-assisted communication technologies in a composite fading environment.

The second category of research introduces a dual role for UAVs as both RIS carriers and active relays. In [36], a swarm of RIS-equipped UAVs simultaneously transmit signals to a BS to serve multiple Internet of Things (IoT) ground nodes. The authors maximized the total rate of the nodes while minimizing the user data rate difference by jointly optimizing the trajectory and phase shift matrices, and simulated to verify the results and accuracy of the proposed model. Qi *et al.* [37] investigated UAV-RIS-assisted vehicular networks, in which UAVs act as dual roles of mobile relays and RIS carriers. The average age of information (AoI) of the system is minimized by jointly optimizing the phase shift of the RIS, the spectrum allocation, and the UAV trajectory.

The third category represents a mainstream of current research, where existing studies concentrate on the downlink communications between UAVs and ground users, utilizing a RIS as a passive relay. RIS-assisted dynamic UAV downlink communication networks were studied in [38]. All user and rate maximization was accomplished based on block coordinate descent. UAV trajectory optimization was accomplished based on augmented reinforcement learning. The proposed algorithm obtains effectiveness and high performance gain compared to other benchmark schemes. In [39], the authors designed a UAV-based wireless network with wireless access and backhaul links utilizing RIS. The design aims to maximize the total rate achieved by ground users by optimizing UAV placement, RIS phase shifting, and subchannel allocation that takes into account wireless backhaul capacity constraints. The effectiveness of the proposed design is demonstrated through an extensive numerical study. A UAV-based multiple RIS network is investigated in [40], in which a hovering UAV acts as a base station and RIS enhances the over-the-barrier signaling between the user and the UAV. In order to achieve the maximum total rate for the proposed communication scenario, the non-convexity problem considering the RIS correlation results, the UAV hovering height, and the multi-RIS phase-shift design is solved. The proposed scenario is superior to the baseline scenario comparing various network settings.

According to the above survey, the existing optimization objectives for the joint use of UAV and RIS mainly focus on the physical layer performance parameters of the system downlink. Based on the results of our search, there is no existing research on the joint use of UAV and RIS for uplink and device-to-device (D2D) link MAC protocol design, especially

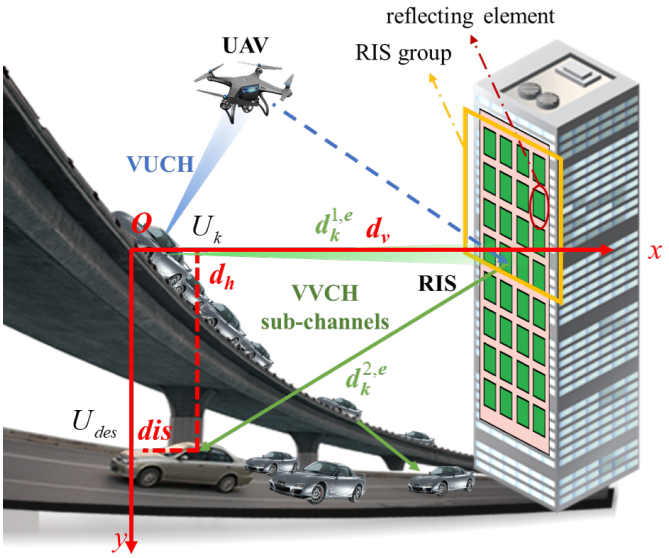

Fig. 2. Details inside a traffic cell.

in vehicular communication scenarios. In the current study, the focus of the joint optimization problem is not on system performance such as system capacity and message delay when UAV and RIS are used together.

However, there are still some challenges in utilizing both UAV and RIS at the MAC layer for multi-ICV user transmissions, e.g., a) how to construct UAV-enhanced RIS-assisted communications for multi-ICV V2X systems; b) how to avoid interference caused by RIS reflections at the receiver side; c) how to optimize the RIS configurations to obtain MAC-layer performance enhancements. To the best of our knowledge, these problems cannot be solved by directly applying existing MAC schemes.

1) To address challenge a), we design a new UAV-enhanced RIS-assisted V2X architecture in which the core network access and data transmission of ICVs are combined in a hybrid manner. In the message report phase, each ICV user reports information to the core network via a UAV acting as an AP. In the transmission competition phase, RIS-assisted transmission resources are acquired. This design is particularly suitable for IoV systems seeking spectral efficiency.
2) To address challenge b), we design a resource reservation scheme for each ICV user. Each user can reserve RIS resources in advance by sending a request to the UAV to realize RIS-assisted multiple data transmissions on the VVCH without interference, thus improving the utilization of RIS elements.
3) To address challenge c), we formulate a joint optimization problem for RIS-assisted communication that considers RIS configuration, transmission power, and MAC parameters to maximize system capacity.

III. System Model

As shown in Fig. 1, the V2X application scenario considered in this paper is an urban traffic section with a considerable number of buildings and overpasses. RISs are deployed at certain intervals on the surface of buildings next to the road. When the traffic section generates congestion or other abnormal emergencies, we deploy several rotary-wing UAVs at certain intervals over the section. The traffic section is divided into multiple cells as shown in Fig. 2. Each cell is equipped with a RIS, a hovering UAV, and multiple ICVs. The UAV can communicate with all ICVs located in the cell when unobstructed. Each ICV is equipped with a GPS device to obtain its real-time location, speed, and direction information.

To simplify the scenario, the following assumptions are made.

1) All ICVs are one-hop nodes that can only send and receive signals with their one-hop neighbors.
   This assumption is made to simplify the system design and frame structure design. In this paper, V2V communication is not multi-hop forwarded, which avoids the impact of routing protocol selection on system performance. Consequently, the system performance is only affected by the protocol flow design and RIS reflection.
2) The dedicated phase configure module of the UAV controls the RIS controller attached with the RIS via a separate wireless link.
   This assumption is made to allow the UAV to control the RIS controller in real time based on the calculation of the RIS phase shift matrix to assist the V2V communication. The basis for this assumption can be found in [41] and [42].

The definitions of variables and constants in this paper are given in Table I. There are following three types of channels in the proposed V2X architecture.

1) **ICV-UAV channel (VUCH)**: the only channel between the ICVs and the UAV in a traffic cell, denoted by c_0. First, the ICVs use VUCH to periodically report driving information to the UAV, which in turn periodically broadcasts safety and road condition information to the ICVs. Meanwhile, the ICVs access the core network through the UAVs. Second, VUCH is used by ICVs to compete for resources reserved for RIS-assisted communication with other ICVs allocated by UAVs.
2) **ICV-ICV channel (VVCH)**: M channels between ICVs and RIS or other ICVs are ICV-ICV channels (VVCH), denoted by $c_1, c_2, ..., c_M$. VVCH is used for the transmission of application messages between ICVs. One ICV provides service on a certain VVCH sub-channel reserved for it by the UAV, while the other receives it.
3) **UAV-UAV channel (UUCH)**: the channel between the UAVs in neighbor cells is UUCH, denoted by c_U. UUCH is used to exchange necessary road and ICV information between UAVs in neighboring cells.

The RIS is composed of N passive elements. The elements can be divided into L groups with $E = N/L$ elements in each group. The L groups are assigned to M sub-channels of VVCH ,which support the communication behavior of K users (i.e., $U_k, k \in [1, K]$). We set $L = M$ for simplicity.

The number of time slots in the message report phase of the VUCH which is presented in section IV is associated with

the group number of the RIS. The probability that an ICV in the cell has a RIS-assisted V2V transmission requirement is assumed to be p_{V2V}. The number of time slots in the message report phase is denoted by N_{slot}, which can be calculated as $N_{slot} = \left\lceil \frac{K_{\max}}{p_{V2V}} \right\rceil$. $K_{\max}$ is the maximum number of ICV users with V2V transmission requirements supported by the cell. Assuming that the communication capacity of each user is sufficient, then $K_{\max}$ increases with the increase of L. To facilitate the calculation, we set that the minimum value of K_{max} is $K_{\max,\min} = 25$ when $L = 1$. The value of K_{max} taken for different L can be computed as $K_{\max,L} = L \cdot K_{\max,\min}$.

$R_{k,eff}$ denotes the effective information rate of each ICV, which is set to 200kbps in this paper. The achievable data rate per ICV on the VVCH can be expressed as

$$R_k(\rho_k, \phi_k) = (B/M)\log_2(1 + \mathrm{SNR}_k)\, t_{V2V}/T_{VVCH}. \quad (1)$$

Each ICV is equipped with two transceivers. Transceiver 1 is always tuned to the VUCH, while transceiver 2 can be tuned to any sub-channel of the VVCH.

The uplink channel from the source ICV user U_k to the group l of the RIS and the downlink channel from the group l to the destination ICV user U_{des} are denoted as $\mathbf{G}_k^l = \left[G_k^{l(1)}, ..., G_k^{l(e)}, ..., G_k^{l(E)}\right]^{\mathrm{T}}$ and $\mathbf{H}_k^l = \left[H_k^{l(1)}, ..., H_k^{l(e)}, ..., H_k^{l(E)}\right]$, respectively. The direct channel from U_k to U_{des} is denoted by h_k.

The received signal at the ICV U_{des} can be expressed as $y_k = (h_k + \mathbf{H}_k^l \mathbf{\Theta}_k^l \mathbf{G}_k^l) x_k + w_k$, where x_k represents the signal transmitted by U_k, w_k represents the additive white Gaussian noise (AWGN) of U_k at U_{des} with zero mean and variance σ^2, and the phase-shift matrix $\mathbf{\Theta}_k^l$ can be defined as $\mathbf{\Theta}_k^l = diag(\phi_k^{l(1)}, \ldots, \phi_k^{l(e)}, \ldots, \phi_k^{l(E)})$.

The phase shift of the element e on the group l can be expressed as

$$\phi_k^{l(e)} = \left\{ \phi_k^{l(e)} \mid \phi_k^{l(e)} = \exp\left(j\theta_k^{l(e)}\right), \theta_k^{l(e)} \in \mathbf{\Omega}, \forall e \in [1, E] \right\}, \quad (2)$$

where $\theta_k^{l(e)}$ is the phase shift reflection coefficient of element e. $\mathbf{\Omega} = \{0, \Delta\theta, \ldots, \Delta\theta(\Psi - 1)\}$ denotes the phase shifts set. Considering the hardware implementation, here we assume that the amplitude reflection coefficient is constant. The number of bits used for each level is denoted by b, giving a total of $\Psi = 2^b$ levels. Dividing 2π into Ψ levels gives $\mathbf{\Omega} = \{0, \Delta\theta, \ldots, \Delta\theta(\Psi - 1)\}$. In order to recover the same reflected signal as the transmitted signal, the RIS controller carried by the UAV adjusts the reflection coefficient of the RIS to achieve a coherent summation of the signals at U_{des}.

The signal-to-noise ratio for RIS-assisted V2V communication can be calculated as

$$\mathrm{SNR}_k = \left| \left(h_k + \mathbf{H}_k^l \mathbf{\Theta}_k^l \mathbf{G}_k^l\right) \rho_k \right|^2 / \sigma^2. \quad (3)$$

IV. UR-V2X-MAC Protocol

In this section, we give the process of UR-V2X-MAC protocol in Algorithm 1, which details the implementation of V2U communication and V2V communication. Five packet structures used in the protocol are presented.

TABLE I
Simulation Parameters Setting

Parameter	Destination	Value
v	the average speed of ICVs	30km/h
m	the maximum backoff stage	10
W_0	the size of the initial contention window	32
l_{cell}	the length of a cell	500m
R_{VUCH}	the bit rate of the VUCH channel	3Mbps
T_{DTR}	the duration of DTR	85μs
T_{DTP}	the duration of DTP	64μs
T_{SIFS}	the duration of SIFS	10μs
T_{DIFS}	the duration of DIFS	50μs
σ	the duration of an idle time slot	20μs
λ	the packet arrival rate	50packets/s
$size(packet_{V2V})$	the size of a data packet	32kb
$size(message_{V2V})$	the size of a V2V message	192kb
t_{V2V}	the size of the time slot on the VVCH	8ms
T_{VUCH}	the length of the time frame on the VUCH	200ms
T_{VVCH}	the length of the time frame on the VVCH	200ms
B_{VVCH}	the total bandwidth of the VVCH	60MHz

A. Implementation of V2U Communication

As shown in Fig. 3, time is divided into frames on the VUCH. Each frame is divided into a message report phase and a transmission competition phase. As shown in Phase 1 in Algorithm 1, the ICVs send message report packets (MRPs) to the UAV at their respective slots to report their travel information in the message report phase. After receiving the packets inerrably, the UAV returns acknowledgments (ACKs) and stores the messages, then predicts the real-time position of each ICV before its next report. In the last slot of this phase, the UAV uses all the messages received during this phase to estimate the road condition and broadcast the result to all ICVs within its coverage area.

When U_k wants to join a cell and access a time slot in the message report phase, it first senses a complete VUCH frame and stores the idle time slot index into the set $\beta(x)$. In the next VUCH frame, U_k selects a random time slot from $\beta(x)$ to send an MRP to the UAV.

If only U_k attempts to send within this slot, it successfully occupies the slot and the UAV returns an ACK with the slot index to it. If the UAV detects a collision within this time slot, it means that at least two ICVs are trying to access this slot at the same time. All ICVs that send an MRP but do not receive an ACK with the index reselect the time slot in the next frame until the slot is successfully acquired.

B. Implementation of V2V Communication

As shown in Phase 2 in Algorithm 1, ICVs with V2V data transmission demand compete for access to the VUCH channel by sending data transmission requests (DTRs) to the UAV in the transmission competition phase on the VUCH. After receiving and parsing the DTR, according to the length of the application and the location of the destination, the UAV reserves multi-dimensional resources for the successful ICV and controls the RIS elements to assist the transmission. Then it returns a data transmission permission (DTP) to the successful ICV to announce the reserved resources. The ICV that receives the DTP starts the RIS-assisted transmission on the VVCH using the reserved resources.

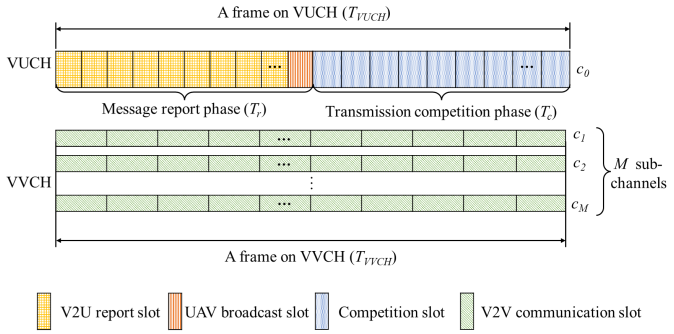

Fig. 3. The time frame structure of UR-V2X-MAC.

Suppose that U_k needs to transmit data to U_{des}. U_k will indirectly compete for RIS-assisted V2V transport resources by using modified CSMA/CA to compete for VUCH access. The following process will be executed.

1) **Compete**. U_k monitors the VUCH activities on the transmission competition phase until it detects an idle period equivalent to a distributed interframe space (DIFS). Once a DIFS is sensed, U_k introduces a random backoff interval before transmitting. The backoff time counter decreases in terms of slot time as long as the VUCH remains idle. When a transmission is detected on the VUCH, the counter freezes, and it resumes counting down when the VUCH is idle again for more than a DIFS. Once the backoff time reaches 0, U_k initiates a transmission by sending a DTR. The backoff time for each transmission is uniformly chosen from the range of $[0, CW-1]$, where CW represents the backoff window size of U_k.
2) **Reply**. The UAV parses the DTR after receiving it. First, the UAV obtains the current position of U_{des} based on the address-location correspondence table it stored, to determine whether U_{des} is within the current cell. If it is within the current cell, a transmission resource reservation is made for U_k directly based on the application size. Subsequently, a DTP is returned to U_k informing of the reserved resources. If it is not within the current cell, the UAV transmits the relevant information in the DTR to the neighboring cell UAV on the UUCH. Subsequently, the DTP from the neighboring cell UAV with the reserved resources is relayed to U_k via the current UAV.
3) **Transmit**. As shown in Fig.3, time is similarly divided into frames on the sub-channels of the VVCH. Each frame can be further divided into multiple time slots. When receives the DTP back from the UAV, it stops competing on the VUCH. U_k parses the DTP and tunes the other transceiver to the VVCH sub-channel allocated for it by the UAV. The UAV and U_k maximizes the system capacity by alternately optimizing the transmit power and the phase shift matrix of the RIS. The RIS phase shift matrix is remotely adjusted so that it accurately reflects the signal from U_k to U_{des}. U_k starts a RIS-assisted transmission to U_{des} in the time slot allocated to it by the UAV. At the end of the

Algorithm 1: Communications with UR-V2X-MAC.

Input: M, L
Output: $t_k, \phi_k^l, \rho_k^2, c_k, l_k$
1: Initialize $\left|\phi_k^l\right| = 0, \rho_k^2 = P, j, k \in [1, K]$
2: $t = 0$;
3: U_k senses a complete frame on VUCH;
4: U_k stores a set of idle time slots $\beta(x)$
5: U_k selects a slot t_k in $\beta(x)$ to send MRP to UAV;
6: UAV receives MRP and judges;
7: **if** no collision **then**
8: UAV replies ACK to U_k;
9: U_k sets t_k as its message report slot on VUCH;
10: **else**
11: UAV replies ACK without indexes of any slots;
12: Go back to line 5;
13: **end if**
14: U_k receives ACK and waits for **Phase 1** arriving;
15: **Phase 1**: **Message Report Phase on VUCH**;
16: **if** t is in **Phase 1 then**
17: U_k sends MRP to UAV in the slot t_k;
18: UAV receives MRP and replies ACK to U_k;
19: **else**
20: U_k waits for **Phase 1** arriving;
21: **end if**
22: **Phase 2**: **Transmission Competition Phase on VUCH**;
23: **if** t is in **Phase 2 then**
24: **if** U_k has data to transmit to another user **then**
25: U_k sets its backoff value s, w;
26: **if** $w = 0$ **then**
27: U_k sends DTR to UAV;
28: $U_{j,j\neq k}$ sets NAV and keeps silent;
29: UAV receives DTR and judges;
30: **if** no collision **then**
31: UAV calculates ϕ_k^l, ρ_k^2, l_k;
32: UAV modifies the RIS controller parameters: ϕ_k^l, l_k, c_k;
33: UAV replies DTP to U_k;
34: **else**
35: UAV replies DTP without reservation to U_k
36: **end if**
37: U_k receives DTP and waits for **Phase 2** arriving;
38: **else**
39: $w--$;
40: **end if**
41: **else**
42: U_k keeps silent;
43: **end if**
44: **else**
45: U_k waits for **Phase 2** arriving;
46: **end if**

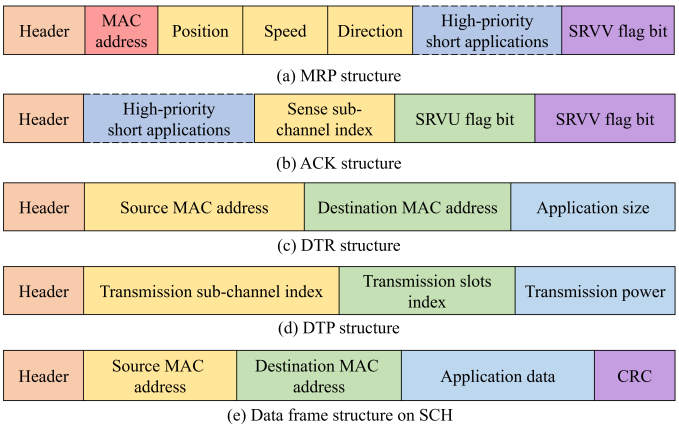

Fig. 4. Structures of packets.

transmission, the RIS group and its corresponding sub-channel are released on the allocated time slot and can be re-reserved by the UAV. At this point, a V2V communication process is complete.

C. Structures of Different Packets

1) **MRP**
The MRP is divided into five main fields: header, MAC address, travel information of the sender, high-priority short applications, and the successful reception on the VVCH (SRVV) flag bit. When the ICV receives the message inerrably on the VVCH, the SRS flag bit is set to 1, allowing the UAV to forward this acknowledgment to the sending ICV when its slot arrives. The format of MRP is shown in Fig. 4(a).
2) **ACK**
The ACK is divided into five main fields: header, high-priority short applications, sense sub-channel index, the successful reception on VUCH (SRVU) flag bit, and SRVV flag bit. The SRVU flag bit is set to 1 when the UAV receives the MRP inerrably on the VUCH. The SRVV flag bit here is set to 1 when the last message sent by the current ICV on the VVCH was successfully received by the receiving ICV. The format of ACK is shown in Fig. 4(b).
3) **DTR**
The DTR is divided into four main fields: header, source MAC address, destination MAC address, and application size. The format of DTR is shown in Fig. 4(c).
4) **DTP**
The DTP is divided into four main fields: header, transmission sub-channel index, transmission slots index, and transmission power. The format of DTP is shown in Fig. 4(d).
5) **Data Packet**
The data frame on VVCH is divided into five main fields: header, source MAC address, destination MAC address, application data and cyclic redundancy check (CRC). The format of the data frame on VVCH is shown in Fig. 4(e).

V. Performance Analysis

In this section, we first model the ICV acquiring time slots in the message report phase as a discrete Markov process, and analyze the probability of successful acquirement. Subsequently, the transmission competition phase is modeled as a Two-state transfer discrete Markov process. We analyze the time required for ICVs to acquire V2V transmission resources. Finally, we model the optimization problem to maximize the system capacity and give the alternating optimization process to solve the problem in Algorithm 2.

A. Message Report Phase Analysis

This section analyzes the speed at which ICVs acquire time slots on the message report phase of the VUCH. An ICV newly entering the current traffic cell tries to acquire a time slot in this phase after listening to a complete frame on the VUCH.

Let D represent the initial number of time slots in this phase, and X_d represent the total number of ICVs that obtain time slots in d frames. X_d is a stationary discrete time Markov process. We use $W(\alpha,\beta,\gamma)$ to represent the number of ways in which α ICVs can obtain time slots. It is assumed that there are β contending ICVs, and each ICV randomly selects a time slot among $gamma$ available time slots. The ICV obtains a slot if no other chooses to access the same one. The probability that the total number of ICVs obtaining time slots in d frames changes from μ to ν can be calculated as

$$P_{\nu|\mu}=\begin{cases}\frac{W(\nu-\mu,K-\mu,D-\mu)}{(D-\mu)^{K-\mu}}, & 0\le\mu\le K-1,\mu\le\nu\le K\\ 1, & \mu=\nu=K\\ 0, & \text{elsewhere}\end{cases} \tag{4}$$

where $W(\nu-\mu,K-\mu,D-\mu)$ denotes the number of ways with $\nu-\mu$ ICVs contending successfully when $K-\mu$ ICVs contend for $D-\mu$ time slots. Under each way, the probability of successful contention is $1/(D-\mu)^{K-\mu}$. $W(\alpha,\beta,\gamma)$ can be calculated as

$$W(\alpha,\beta,\gamma)=\begin{cases}C_\beta^\alpha A_\gamma^\alpha\left((\gamma-\alpha)^{\beta-\alpha}-\sum\limits_{i=1}^{\beta-\alpha}W(i,\beta-\alpha,s-\alpha)\right), & 0\le\alpha<\beta\\ A_\alpha^\gamma, & \alpha=\beta\\ 0, & \alpha>\beta\end{cases} \tag{5}$$

where $(\gamma-\alpha)^{\beta-\alpha}$ calculates the number of ways in which the $\beta-\alpha$ ICVs are allocated to $\gamma-\alpha$ time slots, and $\sum\limits_{i=1}^{\beta-\alpha}W(i,\beta-\alpha,s-\alpha)$ calculates the number of ways in which one-to-one pairings occur when allocating $\beta-\alpha$ ICVs to $\gamma-\alpha$ time slots.

The probability of having X_d ICVs acquiring time slots within d frames can be expressed using the d-step transition probability matrix $\mathbf{P^d}$ as

$$p(X_d=\xi)=\mathbf{P^d}(1,\xi+1),\xi=0,...,K, \tag{6}$$

where $\mathbf{P^d}(1,\xi+1)$ represents the elements of row 1 and column $\xi+1$ of matrix $\mathbf{P^d}$.

The probability of all ICVs acquiring a time slot in d frames can be calculated as

$$F_d^{\text{all}}=p\left(X_d=K\right)=\mathbf{P^d}(1,K+1). \tag{7}$$

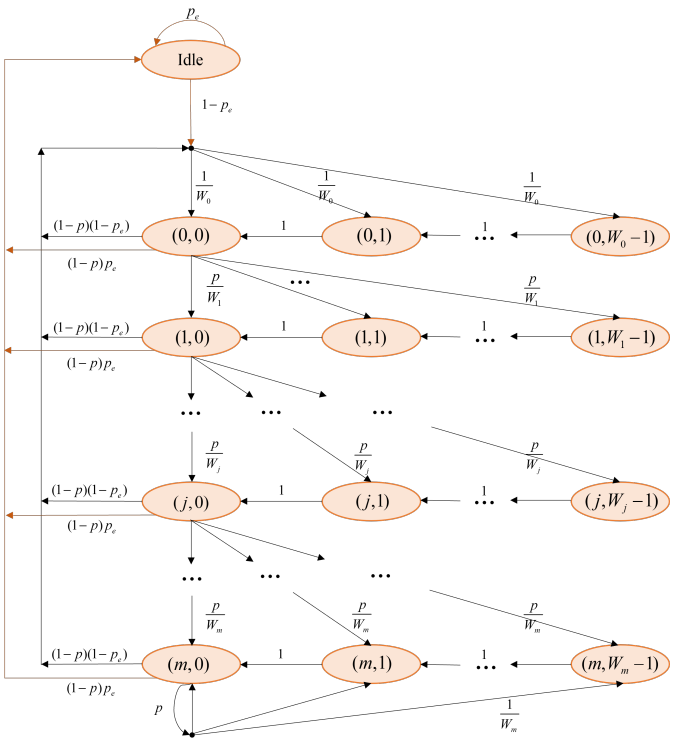

Fig. 5. Two-state transfer discrete Markov model.

The average number of ICVs acquiring a slot within d frames can be calculated as

$$\bar{X}_d = \sum_{\xi=0}^{K} \xi \mathbf{P^d}(1, \xi+1). \tag{8}$$

We express the event that a particular ICV successfully obtains a time slot within d frames by H. The probability of H occurring can be calculated as

$$\begin{aligned} p(H) = F_d &= \sum_{\xi=0}^{K} p\left(H \mid X_d = \xi\right) p\left(X_d = \xi\right) \\ &= \sum_{\xi=0}^{K} \frac{\xi}{K} \mathbf{P^d}(1, \xi+1) = \frac{\bar{X}_d}{K}, \end{aligned} \tag{9}$$

where $p\left(H \mid X_d = \xi\right) = \xi / K$ because of the same probability that each ICV can obtain a time slot.

B. Transmission Competition Phase State Analysis

In this section, we study the behavior of a single ICV with V2V transmission requirements by using the Markov model, and obtain the stationary probability that the ICV transmits data within a slot. Then, we are able to use the computed value to represent the average time required for an ICV with a V2V transmission requirement to acquire a transmission resource. The key approximation that enables our model is the assumption of constant and independent collision probability of a packet transmitted by each ICV, regardless of the number of retransmissions already suffered. As proven by comparison with simulation, this assumption leads to extremely accurate results, especially when the number of stations in the network is fairly large (say greater than ten) [43]. Once independence is assumed, it is possible to model the bi-dimensional process of transmission competition with the discrete-time Markov chain depicted in Fig. 5.

Each ICV during this phase is in one of two states, busy or idle, within a time slot. The probability that each ICV has no demand for V2V transmission, i.e. the probability of being in an idle state, is denoted as p_e. Busy state indicates that the ICV is in contention or in transmission with probability p_{V2V} mentioned in the system model, which can be calculated as $p_{V2V} = 1 - p_e$.

Let $b_{s,w} = \lim_{t\to\infty} P\{s(t) = s, b(t) = w\}, s \in (0, m), w \in (0, W_s - 1)$ be the stationary distribution of the Markov chain, where $s(t)$ and $b(t)$ denote the backoff stage and the value of the backoff counter, respectively. m is the maximum backoff stage. $W_s = 2^s W_0$ is the contention window size for the s_{th} backoff stage. Based on the analysis we can obtain

$$\begin{cases} 1)\ P_{\text{Idle}|\text{Idle}} = p_e, & \\ 2)\ P_{0,w|\text{Idle}} = (1-p_e)/W_0, & w \in [0, W_0 - 1] \\ 3)\ P_{s,w|s,w+1} = 1, & w \in [0, W_s - 2], \\ & s \in [0, m] \\ 4)\ P_{0,w|s,0} = (1-p)(1-p_e)/W_0, & w \in [0, W_s - 1], \\ & s \in [0, m] \\ 5)\ P_{m,w|m,0} = p/W_m, & w \in [0, W_m - 1] \\ 6)\ P_{s,w|s-1,0} = p/W_s, & w \in [0, W_s - 1], \\ & s \in [1, m] \\ 7)\ P_{\text{Idle}|s,0} = (1-p)p_e, & s \in [0, m] \end{cases} \tag{10}$$

where p is the probability of a collision when an ICV user transmits and p_e is the probability that an ICV user has no packets waiting to be sent. 1) indicates the probability that the ICV remains idle. 2) indicates the probability that the ICV changes from idle to busy, i.e. there is a demand for V2V transmission. 3) - 6) indicates transition probabilities in the busy state. 7) indicates the probability that the ICV returns to the idle state after the end of reception.

The probability that an ICV transmits data within a slot is

$$\tau = \sum_{s=0}^{m} b_{s,0}. \tag{11}$$

Based on the fact that the probability of the sum of all states of a Markov chain sums to 1, we have

$$\sum_{s=0}^{m} \sum_{w=0}^{W_s - 1} b_{s,w} + b_{\text{Idle}} = 1, \tag{12}$$

where $b_{s,w}$ can be derived from the following equations

$$b_{s,w} = \frac{W_s - w}{W_s} \begin{cases} (1-p_e)\left[(1-p)\sum_{s=0}^{m} b_{s,0} + b_{Idle}\right] & w \in [0, W_s - 1], \\ & s = 0 \\ p b_{s-1,0} & w \in [0, W_s - 1], \\ & s \in [1, m-1] \\ p(b_{m-1,0} + b_{m,0}) & w \in [0, W_s - 1], \\ & s = m \end{cases} \tag{13}$$

When $w = 0$, $b_{s,0}$ can be calculated by

$$b_{s,0} = \begin{cases} (1-p_e)[(1-p)\sum_{s=0}^{m} b_{s,0} + b_{Idle}] & s = 0 \\ pb_{s-1,0} & s \in [1, m-1] \\ p(b_{m-1,0} + b_{m,0}) & s = m \end{cases} \tag{14}$$

Thus, $b_{s,w}$ can be expressed simply as

$$b_{s,w} = \frac{W_s - w}{W_s} \cdot b_{s,0} \tag{15}$$

The idle state probability can be calculated by

$$b_{Idle} = b_{Idle}p_e + (1-p)p_e \sum_{s=0}^{m} b_{s,0} = \frac{p_e}{1-p_e} b_{0,0} \tag{16}$$

The collision probability p can be calculated as

$$p = 1 - (1-\tau)^{K-1}. \tag{17}$$

τ is the probability that an ICV transmits data within a slot, which can be expressed by (18) at the bottom of this page.

The package-free arrival probability p_e can be calculated as

$$p_e = e^{-\lambda T_{ave}}, \tag{19}$$

where λ represents the average packet arrival rate and T_{ave} is the average time taken for one transmission attempt. The T_{ave} can be obtained by

$$T_{ave} = p_b \left(p_s T_s + (1-p_s)T_c\right) + (1-p_b)\sigma, \tag{20}$$

where σ is the duration of an idle time slot. T_s is the average time required for successful transmission and can be calculated as

$$T_s = T_{\mathrm{DTR}} + T_{\mathrm{SIFS}} + T_{\mathrm{DTP}} + T_{\mathrm{DIFS}} + 2\delta. \tag{21}$$

p_s is the probability of one successful transmission occurring, which can be calculated as

$$p_s = K\tau(1-\tau)^{K-1}. \tag{22}$$

T_c is the average time taken for a transmission in which a collision occurs and can be calculated as

$$T_c = T_{\mathrm{DTR}} + T_{\mathrm{DIFS}}. \tag{23}$$

p_b is the probability that the channel is busy and can be calculated as

$$p_b = 1 - (1-\tau)^{K}. \tag{24}$$

The probability of the ICV successfully transmitting a packet, denoted by p_{succ}, can be calculated as

$$p_{succ} = (1-p)\sum_{i=0}^{m} p^i = 1 - p^{m+1}. \tag{25}$$

Let $E(Stage)$ denotes the average number of the backoff stages. By using conditional probability on p_{succ}, We have

$$E(Stage) = \sum_{i=0}^{m} \frac{ip^i(1-p)}{p_{succ}} = \sum_{i=0}^{m} \frac{ip^i(1-p)}{1-p^{m+1}}. \tag{26}$$

The average number of time slots an ICV needs to experience from the time it has a packet transmission demand to the time it successfully sends a packet is denoted as $E(Slot)$, which can be calculated as

$$E(Slot) = \sum_{i=0}^{m} \frac{p^i(1-p)}{1-p^{m+1}} \sum_{j=0}^{i} \frac{W_j - 1}{2}. \tag{27}$$

The average time $E\left(T_{com}\right)$ required for an ICV with a V2V transmission requirement to acquire a transmission resource can be calculated as

$$E\left(T_{com}\right) = T_{ave} \cdot E(Stage) + \sigma \cdot E(Slot). \tag{28}$$

C. Performance Optimization

The system capacity, denoted by Ω_{Total}, counts the total number of V2V communication bits of K ICV users on M sub-channels within one time frame on the VVCH, i.e., T_{VVCH}. Ω_{Total} can be calculated as

$$\Omega_{\mathrm{Total}} = \sum_{j=1}^{M}\sum_{k=1}^{K} \frac{t_{V2V} R_k\left(\rho_k, \phi_k\right)}{T_{VVCH}} \tag{29}$$

To maximize Ω_{Total}, the phase optimization of the RIS is performed at the UAV and the transmit power is optimized at the transmitter. The two optimizations are performed alternately. The alternating optimization problem is formulated as P1.

C1 and C2 give the constraints on the number of ICV users, RIS groups and sub-channels respectively. C3 is the transmit power constraint for U_k, where *P* indicates the transmit power required for the signal to reach any U_{des} from any U_k without using the RIS and P_{RIS} indicates the hardware static power consumption at the RIS. C4 and C5 constrain the amplitude and phase shift of the RIS group respectively.

The power consumption of the RIS is determined by the characteristics of its reflecting elements, which are responsible for phase shifter the incoming signal. The power consumed by each phase shifter varies depending on its type and resolution. For phase shifter with resolutions of 3, 4, 5, and 6 bits, the average power consumption values are 1.5, 4.5, 6, and 7.8mW, respectively [4], [44]. Therefore, the power dissipated at a RIS consists of N identical reflecting elements can be expressed as $P_{\mathrm{RIS}} = NP_n(b)$, where $P_n(b)$ denotes the power consumption

$$\tau = \frac{2\left(1-2p\right)\left(1-p_e\right)}{\left(1-p_e\right)\left[1-2p+W_0\left(1-p-p(2p)^m\right)\right] + 2p_e\left(1-p\right)\left(1-2p\right)} \tag{18}$$

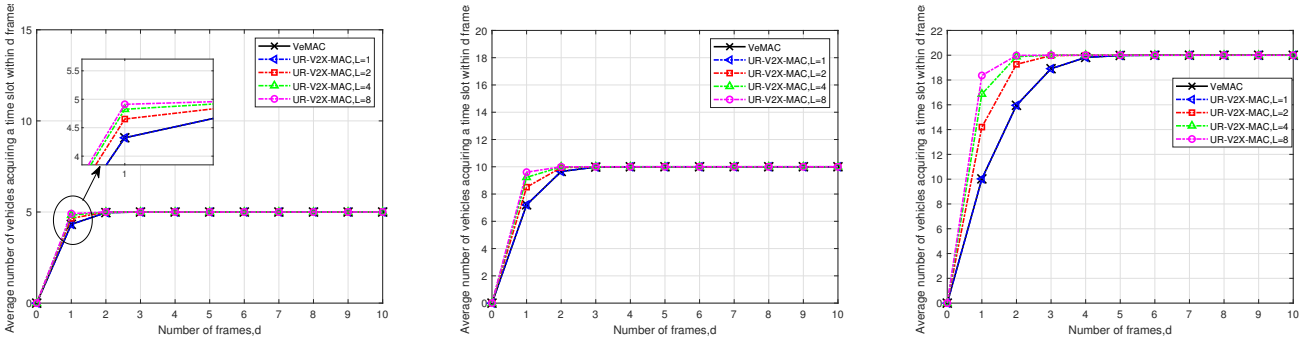

(a) $K_{new} = 5$ (b) $K_{new} = 10$ (c) $K_{new} = 20$

Fig. 6. Average number of ICVs acquiring a slot within d frames, $p_{V2V} = 0.9$.

of each element with b-bit resolution.

$$\begin{aligned} \mathbf{P1}: \quad & \max_{\rho_k^2, \phi_k^{l(e)}} \sum_{k=1}^{K} \Omega_{\text{Total}} \\ \textbf{s.t.} \ \text{C1}: \quad & 1 \le k \le K \\ \text{C2}: \quad & 1 \le l \le L, L = C \\ \text{C3}: \quad & 0 \le \rho_k^2 \le P - \frac{1}{L} P_{\text{RIS}} \\ \text{C4}: \quad & \left|\phi_k^{l(e)}\right| = 1, e \in l \\ \text{C5}: \quad & \theta_k^{l(e)} \in \mathbf{\Omega}, e \in l \end{aligned} \tag{30}$$

We can transform the problem of maximizing the communication capacity in P1 into a problem of maximizing the signal-to-noise ratio at the receiving end. Further, the receiver-side signal-to-noise ratio is maximized by adjusting the phase shift of the elements within the RIS group. According to (1),(3),(29), the optimization problem P1 can be simplified to P2 with the objective of maximizing the signal transmission power:

$$\begin{aligned} \mathbf{P2}: \quad & \max_{\rho_k^2, \phi_k^{l(e)}} \left| \left(h_k + \mathbf{H}_k^l \mathbf{\Theta}_k^l \mathbf{G}_k^l\right) \rho_k \right|^2 \\ \textbf{s.t.} \ & \text{C1}-\text{C5} \end{aligned} \tag{31}$$

To avoid the huge overhead caused by centralized optimization of channel estimation and signal switching, we adopt the distributed optimization algorithm proposed in [20]. The following transformations are made to the variables.

$$\mathbf{H}_k^l \mathbf{\Theta}_k^l \mathbf{G}_k^l \rho_k = \boldsymbol{v}^{\mathrm{H}} \boldsymbol{a} \tag{32}$$

where $\boldsymbol{v} = \left[\phi_k^{l(1)}, \ldots, \phi_k^{l(e)}, \ldots, \phi_k^{l(E)}\right]^{\mathrm{H}}$, and $\boldsymbol{a} = diag(\mathbf{H}_k^l)\mathbf{G}_k^l \rho_k$. $[\cdot]^{\mathrm{H}}$ refers to the conjugate transpose of a matrix. P2 can be simplified as

$$\begin{aligned} \mathbf{P2}': \quad & \max_{\boldsymbol{v}} \boldsymbol{v}^{\mathrm{H}} \boldsymbol{a} \\ \textbf{s.t.} \ \text{C6}: \quad & |v_e| = 1, e \in l \\ \text{C7}: \quad & \arg\left(\boldsymbol{v}^{\mathrm{H}} \boldsymbol{a}\right) = \arg\left(h_k \rho_k\right) \end{aligned} \tag{33}$$

The optimal value for the phase shift of the eth element on group l can be expressed as

$$\theta_k^{l(e)^*} = \arg\left(h_k \rho_k^*\right) - \arg\left(h_k^{l(e)}\right) - \arg\left(g_k^{l(e)} \rho_k^*\right) \tag{34}$$

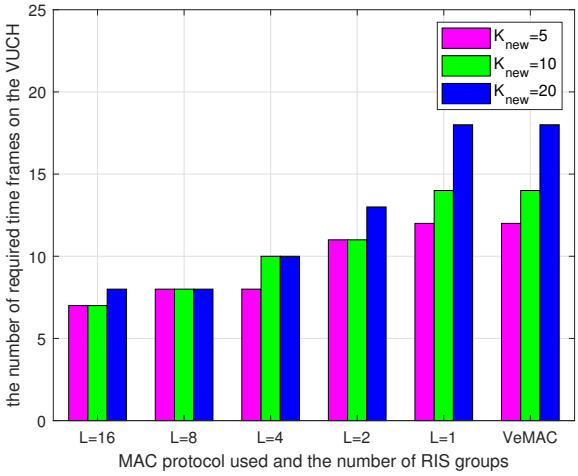

Fig. 7. Number of time frames required to acquire a slot per ICV, p_{V2V}=0.9.

where the channel $g_k^{l(e)}$ represents the transmission path from U_k to the RIS element e within group l, and the channel $h_k^{l(e)}$ represents the transmission path from the RIS element e within group l to U_{des}.

The maximum-ratio transmission (MRT) is the optimal transmit power solution for P1 [45]. The transmit power that maximizes Ω_{Total} at U_k can be expressed as

$$\rho_k^* = \sqrt{P - \frac{1}{L} P_{\text{RIS}}} \frac{h_k + \mathbf{H}_k^l \mathbf{\Theta}_k^{l^*} \mathbf{G}_k^l}{\left|h_k + \mathbf{H}_k^l \Theta_k^{l^*} \mathbf{G}_k^l\right|} \tag{35}$$

The alternating optimization process for UR-V2X-MAC is detailed in Algorithm 2.

VI. Simulation Results

In this section, the delay performance and system capacity performance of the proposed UR-V2X-MAC are simulated. The results are also compared with the existing VANET MAC protocol and the scheme without RIS. Unless otherwise stated, the value settings of significant parameters in the simulation are shown in Table I .

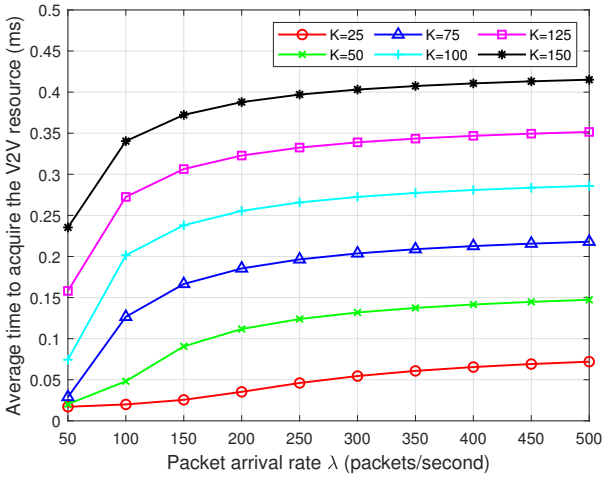

Fig. 8. Average time to acquire the V2V transmission resource versus the packet arrival rate.

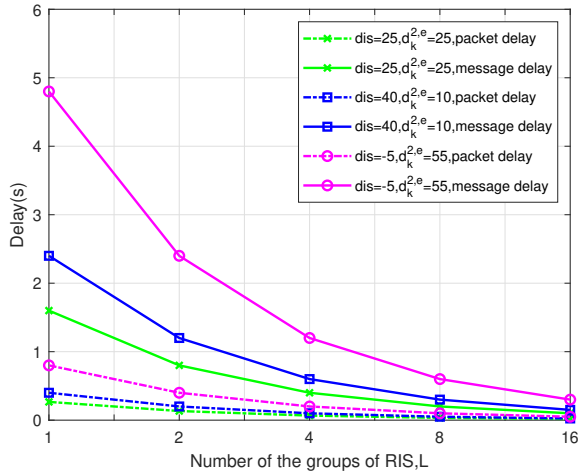

Fig. 9. Delays on the VVCH versus the group number of the RIS, $K = 100, N = 128$.

A. Delay Performance Simulation

We simulate the time taken by the newly added ICVs to acquire time slots in the message report phase. The number of slots N_{slot} within the time frames of the message report phase is associated with the number of groups of RIS L as described in Section III. Fig. 6(a)(b)(c) show the variation of the average number of ICVs acquiring a slot within d frames $\bar{X}_d$ with L for K_{new} = 5, 10, and 20, respectively. From the statistical results it is easy to derive the number of time frames required to acquire one time slot for each ICV when K_{new} = 5, 10, and 20, which is shown in Fig. 7. The analysis of Fig. 6 and Fig. 7 leads to the following conclusions: 1) when using the same MAC protocol with the same parameters, the more competing ICVs there are, the longer it takes to acquire a time slot; 2) when the number of competing ICVs is the same, the time required to acquire a time slot using UR-V2X-MAC is shorter than using VeMAC [5], and the larger L is, the shorter the time required is; 3) the more competing ICVs there are, the more effective it is to reduce the time used to acquire time slots by increasing the L in the UR-V2X-MAC. The reasons for the above observations can be summarized as follows. Since an increase in L expands the amount of available transmission resources, in UR-V2X-MAC we set the total number of time slots in the message report phase to correlate with L, which makes it easier for new joining ICVs to acquire time slots when L increases. The increase in the number of competing ICVs makes this performance improvement particularly obvious. In addition, the simulation results show that there is very little difference in the number of time frames required for ICVs to acquire a time slot in the message report phase when $L = 8$ with K_{new} = 5, 10, and 20. As the number of groups in RIS increases, the overall trend of the number of time frames required for different numbers of new ICVs to join is decreasing, but these decreases are discrete and nonlinear. Therefore, it is reasonable that the number of time frames required for different values of K_{new} are close to each other when L takes a certain fixed value.

Algorithm 2: Optimization of UR-V2X-MAC.

Input: N, L

Output: $\theta_k^{l(e)^*}, \rho_k^*$

Initialize the threshold $\varepsilon > 0$ and the iteration number $\eta = 1$;

The UAV adjusts the RIS to be in receiving mode. U_{des} broadcasts a pilot signal. The RIS estimates phase $\arg\left(h_k^{l(e)}\right)$ and U_k estimates the channel h_k. U_k sets the transmit power as $\rho_{k,\eta} = h_k\sqrt{P - P_{\mathrm{RIS}}/L}\Big/|h_k|$;

if the fractional increment of the objective value is above ε **then**

The UAV adjusts the RIS to be in receiving mode. U_k broadcast a pilot signal with transmit power ρ_k. The RIS estimates phase $\arg\left(g_k^{l(e)}\rho_k\right)$ and computes the phase shift $\theta_{k,\eta+1}^{l(e)}$ by using (34) with given $\rho_{k,\eta}$;

The UAV adjusts the RIS to be in reflecting mode with $\theta_{k,\eta+1}^{l(e)}$. U_{des} broadcasts a pilot signal. U_k estimates the composite channel $h_k + \mathbf{H}_k^l \boldsymbol{\Theta}_k^{l\,*} \mathbf{G}_k^l$ and computes the new transmit power $\rho_{k,\eta+1}$ by using (34) with given $\theta_{k,\eta+1}^{l(e)}$;

$\eta = \eta + 1$;

end if

The average time $E(T_{com})$ required for an ICV with a V2V transmission requirement to acquire a transmission resource varies with the packet arrival rate λ as shown in Fig. 8. It can be observed that $E(T_{com})$ rises slowly as λ increases. When λ is fixed, the more ICVs with V2V transmission requirements, the longer the average time required. V2V data transmission can be performed on VVCH subchannels while competing for transmission resources.

In the scenario illustrated in Fig. 11, we give the following definition.

- dis: the horizontal V2V distance between U_k and U_{des}. A negative value of dis represents the projection of the

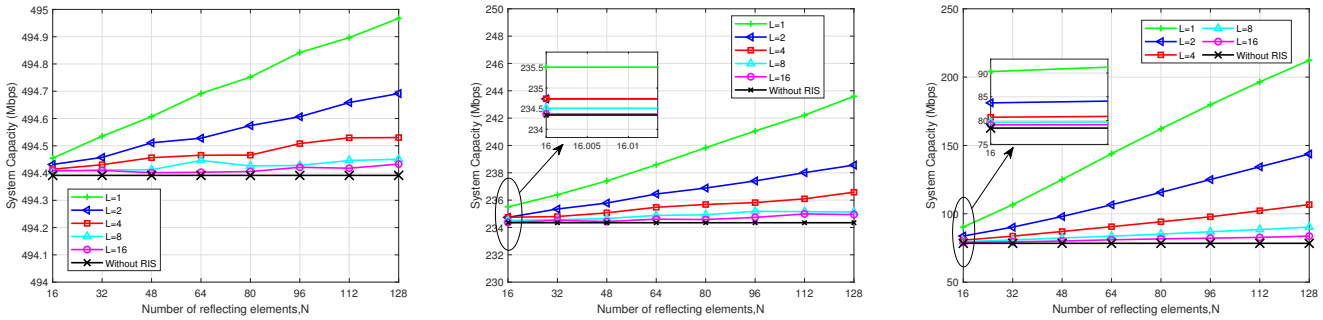

(a) $dis = -5\text{m}$, $d_k^{2,e} = 55\text{m}$ (b) $dis = 25\text{m}$, $d_k^{2,e} = 25\text{m}$ (c) $dis = 40\text{m}$, $d_k^{2,e} = 10\text{m}$

Fig. 10. System capacity versus the number of reflecting elements.

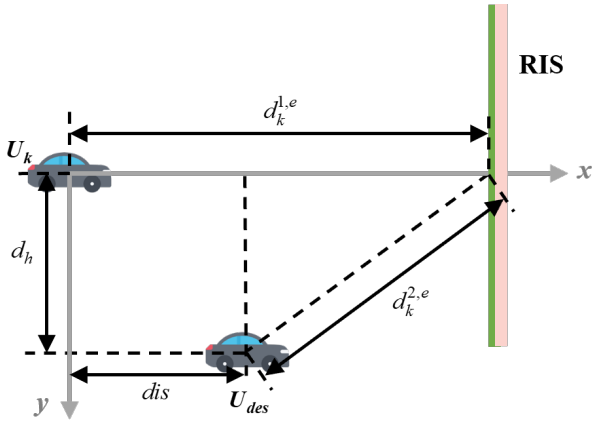

Fig. 11. Simulated RIS-assisted V2V communication scenario.

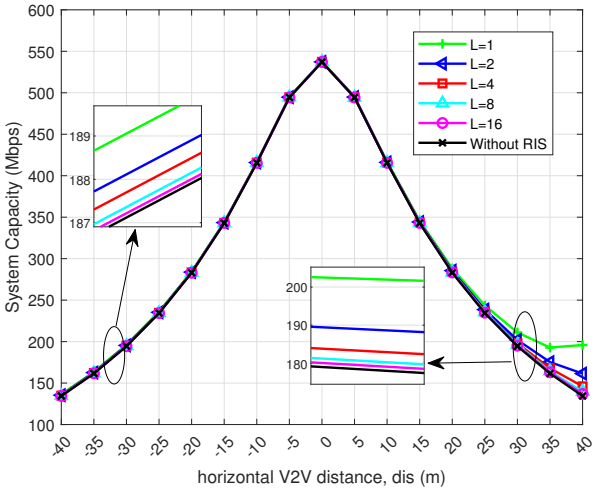

Fig. 12. System capacity versus the horizontal V2V distance, $N = 128$

position of U_{des} in the x-axis direction on the negative half-axis.

- d_h: the vertical V2V distance between U_k and U_{des}. d_h is set to 8m.
- $d_k^{1,e}$: the distance between U_k and the RIS. $d_k^{1,e}$ is set to 50m.
- $d_k^{2,e}$: the distance between the RIS and U_{des}. $d_k^{2,e} = \sqrt{\left(d_k^{1,e} - dis\right)^2 + d_h^2}$.

In Fig. 9, simulation results for V2V transmission packet delay and message delay under dis = -5m, 25m, and 40m ($d_k^{2,e} = 55$m, 25m, and 10m, respectively) are given when the number of RIS elements $N = 128$, and the number of ICVs K with V2V transmission requirements is set to 100. The results for the scheme without RIS are the same as for the $L = 1$ scheme. It can be observed that increasing L significantly reduces the V2V packet delay and message delay, especially in the case that $d_k^{2,e}$ is large. Because when the total number of serving ICV users is constant, the average transmission period required for a single user decreases as L increases with more available transmission resources, assuming sufficient user data bandwidth.

B. System Capacity Performance Simulation

In Fig. 10(a)(b)(c), the variations of the system capacity Ω_{Total} with the number of RIS reflecting elements N are displayed for dis = -5m, 25m, and 40m ($d_k^{1,e}$=55m, 25m, and 10m, respectively). The following conclusions can be drawn from the observations: 1) Ω_{Total} is increasing with N under certain distance parameters when RIS is included in UR-V2X-MAC. The larger L is, the slower Ω_{Total} increases with N; 2) when different combinations of values are taken for N and L, Ω_{Total} of UR-V2X-MAC is always larger than the access scheme without RIS; 3) when dis and N take constant values, the larger L is, the smaller Ω_{Total} is; 4) when the projection of the U_{des} position lies on the positive semiaxis of the x-axis, the larger dis is, the smaller Ω_{Total} is for the same combination of N and L values, whereas the rate of increase of with N is larger. In other words, the decrease of Ω_{Total} with the increase of L is not significant when dis is short. The reasons for the above observations can be summarized as follows. An increase in N leads to more elements receiving the signal energy from U_k, resulting in an array gain of N. It is worth noting that, unlike conventional MRT beamforming using N active antennas that can only obtain a beamforming

gain of N, passive beamforming with RIS can obtain a total beamforming gain of N^2. Consequently, UR-V2X-MAC is more spectrum and energy efficient than ordinary transmission schemes without RIS.

To figure out the relationship between the variation of the system capacity with the V2V distance, we perform the simulation of Fig. 12, i.e., simulate the variation of Ω_{Total} with dis under different schemes and different values of L in UR-V2X-MAC. It can be observed Ω_{Total} increases and then decreases as U_{des} moves in the positive direction along the x-axis and reaches its maximum when U_{des} is directly below U_k. Ω_{Total} of UR-V2X-MAC is always larger than that of the scheme without RIS, even in the scenario where U_{des} is at a distance from the RIS. If dis is large and a scheme without RIS is used, Ω_{Total} will suffer more losses due to signal attenuation. The introduction of RIS in UR-V2X-MAC can well avoid this loss, especially when being deployed closer to the road. In addition, RIS can provide an indirect communication link when there is no LoS path at all between U_k and U_{des}, realizing a non-zero system capacity.

VII. Conclusion

In this paper, we propose a UR-V2X architecture and design a UR-V2X-MAC protocol compatible with it, aiming to solve the challenges of high information delay and insufficient system capacity posed by urban 3D IoT traffic with the rapid development of IoV under the B5G/6G era. Simulation results show that the proposed UR-V2X-MAC has obvious advantages in terms of ICV joining cell delay and V2V transmission delay compared to VeMAC. Meanwhile, UR-V2X-MAC achieves the maximum system capacity enhancement with low complexity through the distributed alternating optimization method, which achieves a significant increase in system capacity compared to the scheme without RIS. Moreover, it is feasible to sacrifice less system capacity in exchange for a reduction in data delay using an increased number of RIS groups, provided that the ICV data bandwidth is sufficient.

In future work, how to balance the system capacity and delay by dynamically adjusting the RIS parameters, transmission parameters, and other reserved resources to further enhance the adaptability of the MAC protocol to 3D urban traffic will be the focus of our research.

References

[1] E. Moradi-Pari, D. Tian, M. Bahramgiri, S. Rajab, and S. Bai, "Dsrc versus lte-v2x: Empirical performance analysis of direct vehicular communication technologies," *IEEE Transactions on Intelligent Transportation Systems*, vol. 24, no. 5, pp. 4889–4903, 2023.

[2] Z. Liu, J. Weng, J. Guo, J. Ma, F. Huang, H. Sun, and Y. Cheng, "Pptm: A privacy-preserving trust management scheme for emergency message dissemination in space–air–ground-integrated vehicular networks," *IEEE Internet of Things Journal*, vol. 9, no. 8, pp. 5943–5956, 2022.

[3] Y. He, D. Wang, F. Huang, R. Zhang, and J. Pan, "Trajectory optimization and channel allocation for delay sensitive secure transmission in uav-relayed vanets," *IEEE Transactions on Vehicular Technology*, vol. 71, no. 4, pp. 4512–4517, 2022.

[4] C. Huang, G. C. Alexandropoulos, A. Zappone, M. Debbah, and C. Yuen, "Energy efficient multi-user miso communication using low resolution large intelligent surfaces," in *2018 IEEE Globecom Workshops (GC Wkshps)*, 2018, pp. 1–6.

[5] H. A. Omar, W. Zhuang, and L. Li, "Vemac: A tdma-based mac protocol for reliable broadcast in vanets," *IEEE Transactions on Mobile Computing*, vol. 12, no. 9, pp. 1724–1736, 2013.

[6] W. Wei, J. Wang, Z. Fang, J. Chen, Y. Ren, and Y. Dong, "3u: Joint design of uav-usv-uuv networks for cooperative target hunting," *IEEE Transactions on Vehicular Technology*, vol. 72, no. 3, pp. 4085–4090, 2023.

[7] A. Al-Hilo, M. Samir, C. Assi, S. Sharafeddine, and D. Ebrahimi, "Uav-assisted content delivery in intelligent transportation systems-joint trajectory planning and cache management," *IEEE Transactions on Intelligent Transportation Systems*, vol. 22, no. 8, pp. 5155–5167, 2021.

[8] Z. Su, M. Dai, Q. Xu, R. Li, and H. Zhang, "Uav enabled content distribution for internet of connected vehicles in 5g heterogeneous networks," *IEEE Transactions on Intelligent Transportation Systems*, vol. 22, no. 8, pp. 5091–5102, 2021.

[9] X. Liu, B. Lai, B. Lin, and V. C. M. Leung, "Joint communication and trajectory optimization for multi-uav enabled mobile internet of vehicles," *IEEE Transactions on Intelligent Transportation Systems*, vol. 23, no. 9, pp. 15 354–15 366, 2022.

[10] Y. Zhou, N. Cheng, N. Lu, and X. S. Shen, "Multi-uav-aided networks: Aerial-ground cooperative vehicular networking architecture," *IEEE Vehicular Technology Magazine*, vol. 10, no. 4, pp. 36–44, 2015.

[11] O. S. Oubbati, A. Lakas, F. Zhou, M. Güneş, N. Lagraa, and M. B. Yagoubi, "Intelligent uav-assisted routing protocol for urban vanets," *Computer Communications*, vol. 107, pp. 93–111, 2017.

[12] O. S. Oubbati, N. Chaib, A. Lakas, P. Lorenz, and A. Rachedi, "Uav-assisted supporting services connectivity in urban vanets," *IEEE Transactions on Vehicular Technology*, vol. 68, no. 4, pp. 3944–3951, 2019.

[13] M. Kadadha, H. Otrok, H. Barada, M. Al-Qutayri, and Y. Al-Hammadi, "A stackelberg game for street-centric qos-olsr protocol in urban vehicular ad hoc networks," *Vehicular Communications*, vol. 13, pp. 64–77, 2018.

[14] H. Abualola, H. Otrok, H. Barada, M. Al-Qutayri, and Y. Al-Hammadi, "Matching game theoretical model for stable relay selection in a uav-assisted internet of vehicles," *Vehicular Communications*, vol. 27, p. 100290, 2021. [Online]. Available: https://www.sciencedirect.com/science/article/pii/S2214209620300619

[15] H. Ghazzai, H. Menouar, and A. Kadri, "On the placement of uav docking stations for future intelligent transportation systems," in *2017 IEEE 85th Vehicular Technology Conference (VTC Spring)*, 2017, pp. 1–6.

[16] M. Samir, M. Chraiti, C. Assi, and A. Ghrayeb, "Joint optimization of uav trajectory and radio resource allocation for drive-thru vehicular networks," in *2019 IEEE Wireless Communications and Networking Conference (WCNC)*, 2019, pp. 1–6.

[17] M. Samir, S. Sharafeddine, C. Assi, T. M. Nguyen, and A. Ghrayeb, "Trajectory planning and resource allocation of multiple uavs for data delivery in vehicular networks," *IEEE Networking Letters*, vol. 1, no. 3, pp. 107–110, 2019.

[18] S. Liu, R. Liu, M. Li, Y. Liu, and Q. Liu, "Joint bs-ris-user association and beamforming design for ris-assisted cellular networks," *IEEE Transactions on Vehicular Technology*, vol. 72, no. 5, pp. 6113–6128, 2023.

[19] C. Pan, G. Zhou, K. Zhi, S. Hong, T. Wu, Y. Pan, H. Ren, M. D. Renzo, A. Lee Swindlehurst, R. Zhang, and A. Y. Zhang, "An overview of signal processing techniques for ris/irs-aided wireless systems," *IEEE Journal of Selected Topics in Signal Processing*, vol. 16, no. 5, pp. 883–917, 2022.

[20] Q. Wu, S. Zhang, B. Zheng, C. You, and R. Zhang, "Intelligent reflecting surface-aided wireless communications: A tutorial," *IEEE Transactions on Communications*, vol. 69, no. 5, pp. 3313–3351, 2021.

[21] C. Pan, H. Ren, K. Wang, J. F. Kolb, M. Elkashlan, M. Chen, M. Di Renzo, Y. Hao, J. Wang, A. L. Swindlehurst, X. You, and L. Hanzo, "Reconfigurable intelligent surfaces for 6g systems: Principles, applications, and research directions," *IEEE Communications Magazine*, vol. 59, no. 6, pp. 14–20, 2021.

[22] Y. Chen, Y. Wang, J. Zhang, and M. D. Renzo, "Qos-driven spectrum sharing for reconfigurable intelligent surfaces (riss) aided vehicular networks," *IEEE Transactions on Wireless Communications*, vol. 20, no. 9, pp. 5969–5985, 2021.

[23] Y. U. Ozcan, O. Ozdemir, and G. K. Kurt, "Reconfigurable intelligent surfaces for the connectivity of autonomous vehicles," *IEEE Transactions on Vehicular Technology*, vol. 70, no. 3, pp. 2508–2513, 2021.

[24] Y. Zhu, B. Mao, Y. Kawamoto, and N. Kato, "Intelligent reflecting surface-aided vehicular networks toward 6g: Vision, proposal, and future

directions," *IEEE Vehicular Technology Magazine*, vol. 16, no. 4, pp. 48–56, 2021.
[25] S. Zeadally, M. A. Javed, and E. B. Hamida, "Vehicular communications for its: Standardization and challenges," *IEEE Communications Standards Magazine*, vol. 4, no. 1, pp. 11–17, 2020.
[26] Q. Pan, J. Wu, J. Nebhen, A. K. Bashir, Y. Su, and J. Li, "Artificial intelligence-based energy efficient communication system for intelligent reflecting surface-driven vanets," *IEEE Transactions on Intelligent Transportation Systems*, vol. 23, no. 10, pp. 19 714–19 726, 2022.
[27] R. Mao and G. Mao, "Road traffic density estimation in vehicular networks," in *2013 IEEE Wireless Communications and Networking Conference (WCNC)*, 2013, pp. 4653–4658.
[28] X. Jiang and D. H. C. Du, "Ptmac: A prediction-based tdma mac protocol for reducing packet collisions in vanet," *IEEE Transactions on Vehicular Technology*, vol. 65, no. 11, pp. 9209–9223, 2016.
[29] Y.-H. Yoon and Y.-B. Ko, "Ctmac: A cooperative tdma mac in vehicular ad hoc networks," in *2017 International Conference on Information and Communication Technology Convergence (ICTC)*, 2017, pp. 772–774.
[30] T. Zhang and Q. Zhu, "Evc-tdma: An enhanced tdma based cooperative mac protocol for vehicular networks," *Journal of Communications and Networks*, vol. 22, no. 4, pp. 316–325, 2020.
[31] Y. Deng, D. Kim, Z. Li, and Y.-J. Choi, "Implementing distributed tdma using relative distance in vehicular networks," *IEEE Transactions on Vehicular Technology*, vol. 69, no. 7, pp. 7295–7305, 2020.
[32] B. Shang, H. V. Poor, and L. Liu, "Aerial reconfigurable intelligent surfaces meet mobile edge computing," *IEEE Wireless Communications*, vol. 29, no. 6, pp. 104–111, 2022.
[33] Y. N. Shnaiwer and M. Kaneko, "Minimizing iot energy consumption by irs-aided uav mobile edge computing," *IEEE Networking Letters*, vol. 5, no. 1, pp. 16–20, 2023.
[34] Z. Zhai, X. Dai, B. Duo, X. Wang, and X. Yuan, "Energy-efficient uav-mounted ris assisted mobile edge computing," *IEEE Wireless Communications Letters*, vol. 11, no. 12, pp. 2507–2511, 2022.
[35] P. S. Bithas, G. A. Ropokis, G. K. Karagiannidis, and H. E. Nistazakis, "Uav-assisted communications with ris: A shadowing-based stochastic analysis," *IEEE Transactions on Vehicular Technology*, pp. 1–11, 2024.
[36] G. Iacovelli, A. Coluccia, and L. A. Grieco, "Multi-uav irs-assisted communications: Multinode channel modeling and fair sum-rate optimization via deep reinforcement learning," *IEEE Internet of Things Journal*, vol. 11, no. 3, pp. 4470–4482, 2024.
[37] W. Qi, C. Yang, Q. Song, Y. Guan, L. Guo, and A. Jamalipour, "Minimizing age of information for hybrid uav-ris-assisted vehicular networks," *IEEE Internet of Things Journal*, pp. 1–1, 2024.
[38] X. Zhang, H. Zhang, W. Du, K. Long, and A. Nallanathan, "Irs empowered uav wireless communication with resource allocation, reflecting design and trajectory optimization," *IEEE Transactions on Wireless Communications*, vol. 21, no. 10, pp. 7867–7880, 2022.
[39] M. D. Nguyen, L. B. Le, and A. Girard, "Uav placement and resource allocation for intelligent reflecting surface assisted uav-based wireless networks," *IEEE Communications Letters*, vol. 26, no. 5, pp. 1106–1110, 2022.
[40] Y. Li, H. Zhang, K. Long, and A. Nallanathan, "Exploring sum rate maximization in uav-based multi-irs networks: Irs association, uav altitude, and phase shift design," *IEEE Transactions on Communications*, vol. 70, no. 11, pp. 7764–7774, 2022.
[41] C. Huang, A. Zappone, G. C. Alexandropoulos, M. Debbah, and C. Yuen, "Reconfigurable intelligent surfaces for energy efficiency in wireless communication," *IEEE Transactions on Wireless Communications*, vol. 18, no. 8, pp. 4157–4170, 2019.
[42] X. Cao, B. Yang, H. Zhang, C. Huang, C. Yuen, and Z. Han, "Reconfigurable-intelligent-surface-assisted mac for wireless networks: Protocol design, analysis, and optimization," *IEEE Internet of Things Journal*, vol. 8, no. 18, pp. 14 171–14 186, 2021.
[43] G. Bianchi, "Performance analysis of the ieee 802.11 distributed coordination function," *IEEE Journal on Selected Areas in Communications*, vol. 18, no. 3, pp. 535–547, 2000.
[44] C. Huang, L. Liu, C. Yuen, and S. Sun, "Iterative channel estimation using lse and sparse message passing for mmwave mimo systems," *IEEE Transactions on Signal Processing*, vol. 67, no. 1, pp. 245–259, 2019.
[45] Q. Wu and R. Zhang, "Intelligent reflecting surface enhanced wireless network via joint active and passive beamforming," *IEEE Transactions on Wireless Communications*, vol. 18, no. 11, pp. 5394–5409, 2019.

Yaqi Mao (Graduate Student Member, IEEE) received the B.E. degree from Nanjing University of Posts and Telecommunications, Nanjing, China, in 2021. She is currently pursuing the Ph.D. degree with the School of Electronics and Information, Northwestern Polytechnical University, Xi'an, China.

Her research interests include wireless network and unmanned aerial vehicle (UAV) communications.

Xin Yang (Member, IEEE) received the B.Sc. degree in communication engineering and the M.Sc. degree in electronics and communication engineering from Xidian University, Xi'an, China, in 2011 and 2014, respectively, and the Ph.D. degree in information and communication engineering from Northwestern Polytechnical University, Xi'an, in 2018.

He is an Associate Professor with the School of Electronics and Information, Northwestern Polytechnical University. His research interests include wireless communications and ad hoc networks.

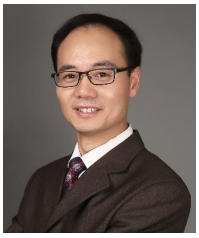

Ling Wang (Member, IEEE) received the Ph.D. degree from Xidian University, Xi'an, China, in 2004.

From 2004 to 2007, he worked with Siemens, Munich, Germany, and Nokia Siemens Networks, Espoo, Finland. Since 2007, he has been with Northwestern Polytechnical University, Xi'an, as a Professor. His current research interests include array processing and smart antennas, wideband communications, cognitive radio, adaptive antijamming for satellite communications, satellite navigation, and date link systems.

Prof. Wang is a recipient of the National Talents Award and he currently serves as the Dean of School of Electronics and Information.

Dawei Wang (Member, IEEE) received the B.S. degree from the University of Jinan, Jinan, China, in 2011, and the Ph.D. degree from Xi'an Jiao Tong University, Xi'an, China, in 2018.

From 2016 to 2017, he was a Visiting Student with the School of Engineering, University of British Columbia, Vancouver, BC, Canada. He is currently an Associate Professor with the School of Electronics and Information, Northwestern Polytechnical University, Xi'an. His research interests include physical layer security, cognitive radio networks, unmanned aerial vehicle (UAV) communications, machine learning, and resource allocation.

Dr. Wang has served as the Technical Program Committee Member for many international conferences, such as IEEE GLOBECOM and IEEE ICC.

Osama Alfarraj (Member, IEEE) received the master's and Ph.D. degrees in information and communication technology from Griffith University, in 2008 and 2013, respectively. He is currently a Professor of computer sciences with King Saudi University, Riyadh, Saudi Arabia. His current research interests include eSystems (eGov, eHealth, and ecommerce), cloud computing, and big data. For two years, he has served as a Consultant and a member for the Saudi National Team for Measuring E-Government, Saudi Arabia.

Keping Yu (Senior Member, IEEE) received the M.E. and Ph.D. degrees from the Graduate School of Global Information and Telecommunication Studies, Waseda University, Japan, in 2012 and 2016, respectively. He was a Research Associate, Junior Researcher, Researcher with the Global Information and Telecommunication Institute, Waseda University, from 2015 to 2019, 2019 to 2020, 2020 to 2022, respectively. He is currently an Associate Professor, the Vice Director of Institute of Integrated Science and Technology, and the Director of the Network Intelligence and Security Laboratory (YU Lab), Hosei University, Japan. He is also a Fellow of the Distinguished Scientist Fellowship Program at King Saud University, Saudi Arabia.

Dr. Yu has hosted and participated in more than ten projects, is involved in many standardization activities organized by ITU-T and ICNRG of IRTF, and has contributed to ITU-T Standards Y.3071 and Supplement 35. He has been a Highly Cited Researcher identified by Clarivate™ (2023) and the World's Top 2% Scientists identified by Stanford University (2022, 2023). He received the Best Symposium Award from IWCMC 2023, the IEEE Outstanding Leadership Award from IEEE BigDataSE 2021, the Best Paper Award from IEEE Consumer Electronics Magazine Award 2022 (1st Place Winner), IEEE ICFTIC 2021, ITU Kaleidoscope 2020, the Student Presentation Award from JSST 2014. He has authored more than 200 peer-review research papers and books, including over 90 IEEE/ACM Transactions papers. He is an Associate Editor of IEEE Open Journal of Vehicular Technology, Journal of Intelligent Manufacturing, Journal of Circuits, Systems and Computers, and IEICE Transactions on Fundamentals of Electronics, Communications and Computer Sciences. He has been a Guest Editor for IEEE Transactions on Computational Social Systems, IEEE Journal of Biomedical and Health Informatics, and Renewable & Sustainable Energy Reviews. He served as general co-chair and publicity co-chair of the IEEE VTC2020-Spring 1st EBTSRA workshop, general co-chair of IEEE ICCC2020 2nd EBTSRA workshop, general co-chair of IEEE TrustCom2021 3nd EBTSRA workshop, session chair of IEEE ICCC2020, ITU Kaleidoscope 2016.

Shahid Mumtaz (Senior Member, IEEE) is an IET Fellow, IEEE ComSoc and ACM Distinguished Speaker, recipient of IEEE ComSoc Young Re searcher Award (2020), founder and EiC of the IET Journal of Quantum Communication, Vice Chair of the Europe/Africa RegionIEEE Com Soc Green Communications Computing Society, and Vice-Chair of IEEE Standard P1932.1: Standard for Licensed/Unlicensed Spectrum Interoperability in Wireless Mobile Networks. He is the author of 4 technical books, 12 book chapters, 300+ technical papers (200+ IEEE journals/transactions, 100+ conference proceedings), and received 2 IEEE best paper awards in the area of mobile communications. Most of his publication is in the field of wireless communication. He is serving as Scientific Expert and Evaluator for various research funding agencies. He was awarded an Alain Bensoussan Fellowship in 2012. He was the recipient of the NSFC Researcher Fund for Young Scientist in 2017 from China.

Fei Richard Yu (Fellow, IEEE) received the PhD degree in electrical engineering from the University of British Columbia (UBC) in 2003. His research interests include connected/autonomous vehicles, artificial intelligence, blockchain, and wireless systems. He has been named in the Clarivate Analytics list of "Highly Cited Researchers" since 2019, and received several Best Paper Awards from some first-tier conferences. He was a Board Member the IEEE VTS and is the Editor-in-Chief for IEEE VTS Mobile World newsletter. He is a Fellow of the IEEE, Canadian Academy of Engineering (CAE), Engineering Institute of Canada (EIC), and IET. He is a Distinguished Lecturer of IEEE in both VTS and ComSoc.